

## The Robonaut 2 Hand – Designed To Do Work With Tools

L. B. Bridgwater\*, C. A. Ihrke\*\*, M. A. Diftler\*, M. E. Abdallah\*\*, N. A. Radford\*, J. M. Rogers\*,  
S. Yayathi\*, R. S. Askew\*, D. M. Linn \*\*

\*NASA/JSC, Houston, Texas

\*\*General Motors, Warren, Michigan,

**Abstract**— The second generation Robonaut hand has many advantages over its predecessor. This mechatronic device is more dexterous and has improved force control and sensing giving it the capability to grasp and actuate a wider range of tools. It can achieve higher peak forces at higher speeds than the original. Developed as part of a partnership between General Motors and NASA, the hand is designed to more closely approximate a human hand. Having a more anthropomorphic design allows the hand to attain a larger set of useful grasps for working with human interfaces. Key to the hand's improved performance is the use of lower friction drive elements and a redistribution of components from the hand to the forearm, permitting more sensing in the fingers and palm where it is most important. The following describes the design, mechanical/electrical integration, and control features of the hand. Lessons learned during the development and initial operations along with planned refinements to make it more effective are presented.

### I. INTRODUCTION

NASA, working with its partner General Motors, developed the Robonaut 2 (R2) hand as a device that could work with a wide range of human interfaces, going beyond the original mandate of using tools designed for Space Walking Astronauts [1]. GM and NASA share the vision of humans and robots working together, with the safety of their people being the overriding priority. In teaming with NASA, GM continued a long standing effort to adapt robotics technology to help their employees perform tasks which currently are ergonomically difficult. From NASA's perspective the GM collaboration was a way to combine resources and expertise to produce a better Robonaut and a much more capable robot hand.

Many advances in dexterous hand technology have been made since the original Robonaut hand was developed in the late 1990s. These are evident in several of the hands developed over roughly the last decade. The three fingered HRP-3 hand provides a significant grasping capability to an impressive walking humanoid [2]. The SSL hand pursues compatibility with a large number of tools through a balance between simplicity and dexterity [3]. The most recent DLR design has moved from an intrinsic to an extrinsic design [4] adding to a series of impressive and capable designs [5],[6].

Like any attempt to recreate the subtleties of human capabilities, in this case, a human hand, this is a work in progress. Important improvements for the R2 hand vs. the

Robonaut 1 hand include increasing the thumb Degrees of Freedom (DoF), overall joint travel, wire reduction and durability. The following describes: design philosophy, mechanism design, sensing, avionics, control, application, lessons learned and future development.

### II. DESIGN PHILOSOPHY

The R2 hand and forearm, shown in Figure 1, are designed to improve upon the approximation of human hand capabilities achieved by its predecessor, Robonaut 1 [1]. The five fingered dexterous hand and forearm is a completely self-contained unit, all motors and avionics are packaged inside the forearm, and only 6 conductors for power and communication from the upper-arm is needed, a huge reduction from the more than 80 conductors of Robonaut 1. This makes the R2 hand an important subsystem of the full humanoid robot and a modular, extremely dexterous, stand-alone end-effector in its own right.

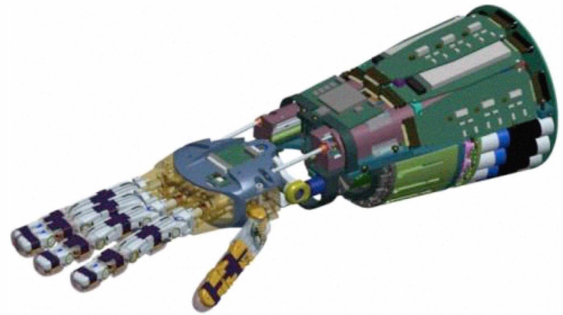


Fig 1. The Robonaut 2 hand and forearm with all avionics

The modularity of the hand continues to the fingers as each of the fingers is treated as an individual sub-assembly. The actuator location and design is also modular allowing for rapid replacement of components and sub-assemblies. Further, the forearm is designed with a quick disconnect from the upper arm allowing for ease of maintenance and assembly.

Simulation is an important tool in evaluating candidate designs. The Cutkosky's grasp taxonomy [7] is an excellent benchmark for evaluating dexterity. While the Robonaut 1 hand could only emulate about 50% of these grasps, the R2 hand design is successful over 90% of the taxonomy [8]. Fig. 2 shows the actual R2 hand emulating 15 of the 16 Cutkosky grasps.



Fig. 2. R2 hand demonstrating the Cutkosky grasp taxonomy

### III. MECHANISM DETAILS

#### A. Overview

The R2 hand and forearm is 127 mm in diameter at its largest and 304 mm long from the base to center of the palm, and has a payload of more than 9 kg. The hand has 12 DoF with a two DoF wrist. Sixteen finger actuators and two wrist actuators in the forearm control the 14 DoF. The fingers can exert a tip force of 2.25 kg while fully extended and a tip speed of more than 200 mm/sec.

The R2 Hand is designed to be comparable in size to a human hand. Hand dimensions are within 60<sup>th</sup> to 85<sup>th</sup> percentile human male [9]. Many design features of the fingers and finger actuation system enable the compact human size of R2's hand while retaining the strength required to work with human tools.

#### B. Finger design

A human finger is generally considered to have four DoF. R2's primary fingers contain four joints, only three of which are independently controllable DoF, configured in such a way as to effectively approximate the poses achievable by the human finger (Fig. 3). The fourth human DoF that is not controllable in this approximation is the distal interphalangeal joint (J4). Rather than independent control, the angle of J4 is a fixed relationship to the proximal interphalangeal joint (J3). The angle is determined by the output of a four-bar linkage consisting of the proximal, medial, and distal phalanges, and a distal linkage is illustrated in Fig. 4.

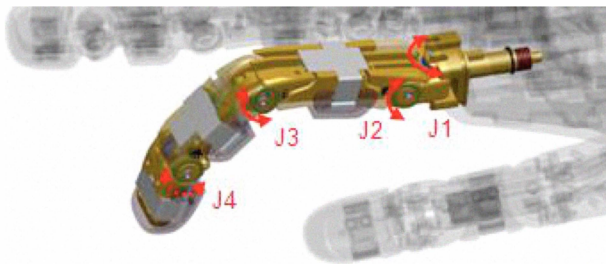


Fig. 3. R2 primary finger with labels and location for each axis

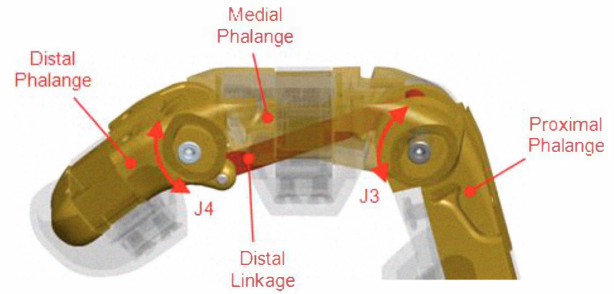


Fig. 4. The angle of J4 dictated by the four bar linkage and the angle at J3

R2's secondary fingers are mechanically similar to its primary fingers except the adduction/abduction of the finger (J1) has been eliminated. Of the remaining three joints, two are loosely coupled, while the third remains linked as described above. The tendons that control the secondary fingers are grounded to the finger at the medial phalange; therefore they produce torque at both the metacarpal interphalangeal joint (J2) and J3.

*Application of the "N+1" Rule* – Minimizing the number of tendons minimizes the space required to accommodate actuation [10]. An N DoF tendon actuated manipulator can be fully controlled by a minimum of N+ 1 tendons. For the primary fingers, i.e. the index and middle fingers, three DoF are fully controlled by four tendons. The secondary fingers, which contain two DoF, are controlled by only two tendons. The secondary fingers are therefore under-actuated and used primarily for grasping, as opposed to dexterous manipulation.

Individual joint travel limits of the fingers are designed to approximate those of a human finger, such that a wide range of comparable poses are achievable. Table I shows the joint ranges of the fingers.

Table I  
Joint range of travel for the R2 fingers

Finger DoF	Range of travel
J1 (Only on primary fingers)	-20° to +20°
J2	-10° to +95°
J3	0° to +120°
J4	0° to +70°

#### C. Thumb design

A human thumb is accurately approximated with five independently controllable degrees of freedom [11]. The R2 thumb contains 4 phalanges and 4 independently controllable DoF which effectively approximate the poses achievable by the human thumb.

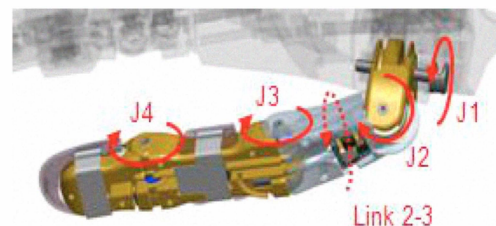


Fig. 5. R2 thumb with labels and location of each axis

The fifth DoF of the human model was the angular twist between the axes of the second and third joints, shown as a dashed arrow in Fig. 5. This DoF has been replaced with a rigid link with a fixed angular twist between J2 and J3. The angle selected was a design trade to most accurately approximate the human thumb opposing to the fingers and accommodate tendon routing. The ranges of motion in the thumb are shown in Table II.

Table II  
Joint range of travel for the R2 thumb

Thumb DoF	Range of travel
J1	0° to +74°
J2	0° to +85°
J3	0° to +90°
J4	-10° to +70°

The thumb also implements an N+1 configuration for control of its four DoF, the selection and routing of the five tendons is chosen to maximize the thumb's ability to oppose the grip-force generated by the four opposing fingers of the hand. Four of the five tendons cross the first two DoF on the flexor side while a single tendon is antagonistic and is shown in Fig. 6.

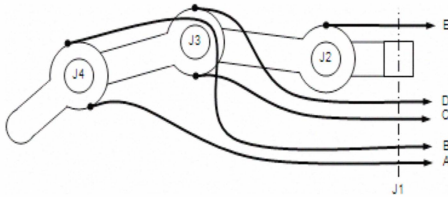


Fig. 6: Tendon routing through the R2 thumb

#### D. Finger Actuators

R2's finger actuation system is a key enabler for compact human size of the fingers of the robotic hand. The components of the actuation system include the actuator (consisting of the motor, gear head and ball screw assembly), tendon, conduit, tension sensor (described below), and terminator (Fig. 7).

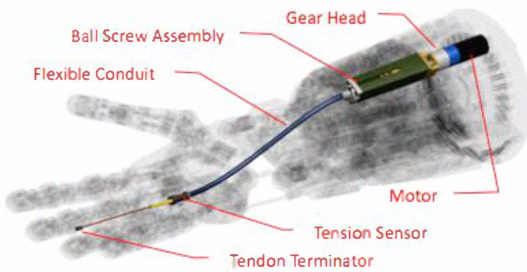


Fig. 7. Actuator system of the R2 hand

The actuator (Fig. 8) is designed for a linear travel of 35 mm and to provide a pulling force of 23 kg. These design values are based on the desired joint ranges and torques required for R2's fingers and thumb.

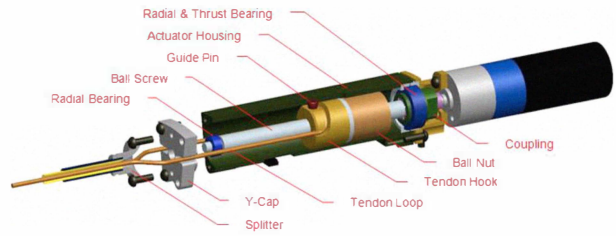


Fig. 8: R2 finger actuator

The tendons used for finger actuation in R2's hand must be mechanically anchored to the bone upon which they exert forces. The space used for this termination is an important consideration. In a new termination method [12], an incompressible ball is placed inside the weave of a hollow-weave braided polymer tendon. The tendon and ball are then placed inside a small cylinder, which captures the ball and lets the tendon pass through the ends of the cylinder. The cylinder contains a feature through which the ball is too large to pass. The assembly is then potted with adhesive to prevent slippage of the ball inside the tendon within the range of design tension loads. This design (Fig. 9) allows for a single continuous tendon to be anchored in the middle, where either end may exert forces on the bone as an antagonistic pair of tendons and reduces the number of terminators needed for each finger. Pairs of tendons in R2's fingers are terminated in a space of 3.1 mm diameter by 5 mm length.

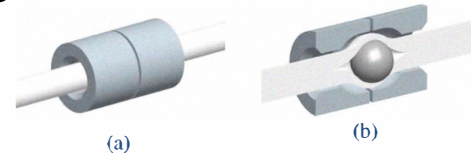


Fig. 9: Tendon terminator (a) assembled and (b) in cross section

**Tendon material** – Through extensive testing Vectran™ was selected for the base tendon material for its strength and resistance to stretch and creep. Its abrasion resistance properties were improved by creating a hybrid weave of Teflon™ with Vectran™. Tendon material of nominal diameter 1.2 mm with break strength of 181 kg, was selected as an optimal balance between size, strength, and abrasion life for the R2 hand.

#### E. Wrist Design

The R2 hand is mounted to the forearm by a universal joint that approximates the human wrist in range of travel. The axes are orthogonal to the forearm roll axis, with the pitch joint proximal and yaw joint distal to the forearm. The axes are separated by 6 mm. The u-joint is attached to the forearm with two shock mounts to absorb impacts as the hand interacts with its environment.

The center of the universal joint is open such that the 16 finger actuator conduits may pass through, in addition to one conduit used to protect wires that must cross the wrist. This routing differs from the human anatomy, but was selected to minimize coupling between finger and wrist motions. Additionally, conduits are layered in a manner that avoids kinking and entanglement during operation.

### F. Wrist Actuator

The R2 wrist is a closed kinematic chain, differentially actuated by two compact linear actuators (Fig. 10) located on the dorsal side of the forearm. These actuators mount to the main forearm bone and follow the tapered shape of the forearm. Each actuator consists of a custom brushless DC motor with a hollow shaft which drives the nut of a ball screw. The screw extends and retracts a slider which drives a ball and socket linkage connected to the palm. Located at the rear, a magnetic incremental encoder tracks the position of the actuator. The wrist actuators can exert a force of 27 kg and have a travel of 100 mm.

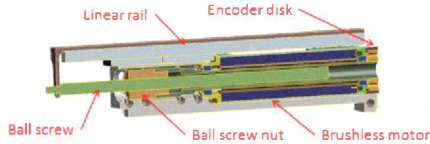


Fig. 10. Wrist actuator assembly

The wrist actuators are attached to the palm through two ball and socket joints on either end of a stainless steel two-force member. The sockets are equipped with bronze cups backed by rubber inserts to allow for favorable wear and shock absorption. The same ball and socket is used on both the actuator and palm sides of the link to ensure commonality of parts and simplicity of manufacturing.

## IV. SENSING

There are three types of sensors in the fingers, thumb and wrist:

### A. Absolute joint position sensing

The absolute angular position of each joint is measured by means of a hall-effect sensor along with a novel “ellipsoidal shaped” magnet [13]. The magnet shape was designed to achieve a linear relationship between angular position and the change in the magnetic field that is measured by the hall-effect read sensor. A circular magnet generates a sinusoidal signal, whereas the novel shape used in R2’s fingers generates an approximately linear signal over a 150° usable range. Fig. 11 shows the magnetic field for the ellipsoidal shaped magnet as compared with a ring magnet.

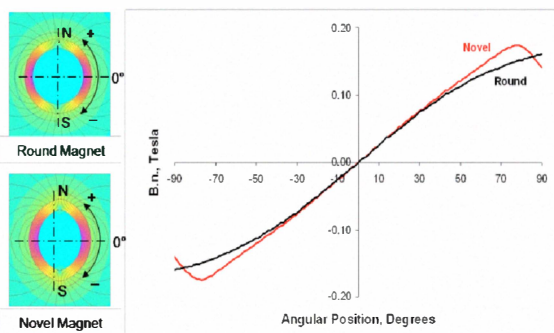


Fig. 11. Comparative magnetic field of the ellipsoidal magnet Vs ring magnet

### B. Tactile load sensing

The proximal, medial, and distal phalanges of the fingers and the medial and distal phalanges of the thumb are each designed to accommodate a phalange tactile load cell, which is a novel six degree of freedom force torque sensor [14].

This load cell evolved from a low profile design (Fig. 12) designed for the base phalange of each finger into an arch that is compatible with all the phalange locations. Each load cell utilizes eight pairs of semiconductor strain gages mounted to an aluminum elastic element. The aluminum strain element is designed to maximize measurable bending strain within the range of design loads, and within the limited space available on the phalanges of the R2 hand. Hard stops redirect the load after approximately 2.2 kg of force or 113 mNm of torque to ensure the strain element does not exceed its elastic limit.

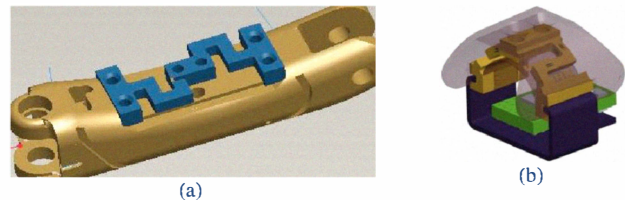


Fig. 12. Evolution of the phalange sensor (a) initial concept, (b) as implemented

### C. Tendon tension sensors

R2’s finger actuation system accommodates sensing of the tension in the tendons by means of a sensor that measures compressive forces in the conduits in which the tendons are routed [15]. It has been found that the measured compressive force in the conduit is equal to the tensile load on the tendon within an error of 5-10%. This error is due to interaction between the conduits within the carpal area as well as friction between the tendon and conduit liner. The tendon tension sensors (Fig. 13) are protected from incidental contact from conduits and objects in the hand by their installation into the structure of the palm.

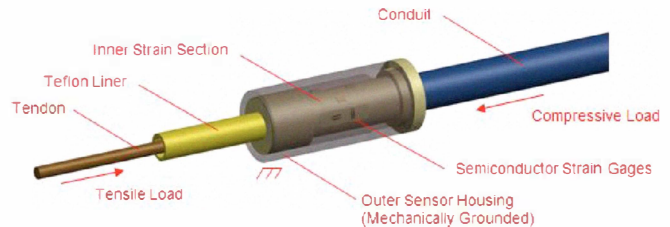


Fig. 13. Anatomy of the tendon tension sensors

## V. AVIONICS AND CONTROLLERS

The forearm contains all the avionics and drive electronics needed for hand operation.

### A. Motor Drivers

Each motor driver “Trident” board (Fig. 14) consists of a custom 3-axis hybrid motor driver, an Actel ProAsic3 FPGA, hall sensor feedback for motor commutation and encoder accumulation, phase current sensing for each motor, and digital temperature channels for the motors and hybrid

drivers. The Actel FPGA on each Trident communicates with the main controller “Medusa” via a point-point serial link. The Trident-Medusa comm. is fully managed in the FPGA fabric and transfers information in parallel with the higher-level Multi Drop Low Voltage Differential Signal (MLVDS) communication. The Trident receives motor PWM commands and provides feedback for the motor phase currents, accumulated encoder position and temperature data back to the Medusa. Current limit thresholds are internally set to provide a level of protection for the motors, actuators, and tendons.

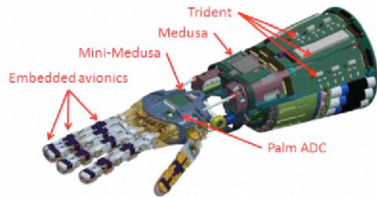


Fig. 14. Location of Medusa and several of the tridents

### B. Main controller

Consistent with the R2 communication system, the MLVDS communication engine in the forearm allows the R2 control system to command and sense all 18 forearm actuators and 50 sensors via a two-wire communication link. The MLVDS and distributed control strategy heavily reduces the conductor count and processor load of the central computer.

The Medusa in the forearm is responsible for communicating with both the R2 brainstem as well as the six Trident boards. The Medusa is primarily comprised of a Xilinx Virtex 4-FX FPGA and a 16 channel analog to digital converter. The MLVDS communication engine that interfaces with the R2 control system is implemented on the FPGA. In initial versions the Virtex 4 FPGA mainly served as a communication distribution hub for the Trident motor drivers, but more recently the onboard PowerPC has been employed to perform all closed loop control for the hand motion. The Medusa reads all finger position and tension sensor data sent through the MLVDS from the hand control processor. In addition the FPGA fabric communicates with the six Trident motor drivers in parallel, and the on board Analog to Digital Converter (ADC), which measures wrist position hall sensors and internal voltages. The Medusa has an SPI Flash memory for storing non-volatile parameters such as control gains or sensor calibration. Available for future use is an IO port for reading one-wire digital temperature sensors.

### C. Sensor Serialization

The FPGA device “Mini-Medusa” located on the dorsal side of the palm controls the serialization of the hand sensor data (Fig. 14). In order to maintain a low conductor count and still process data from 50 different sensors comprised of a total of 164 analog signals, serialization of the sensor chain is necessary.

All of the phalange and angle sensor signals are multiplexed and read by ADCs in the fingers communicate

back to the R2 control system through the Mini-Medusa. Sixteen separate tendon tension sensors are mounted in the palm and each one consists of two half bridges. These signals are routed through a flexible circuit board on the inside of the palm to a flat flex connector on the Palm ADC circuit board. The Palm ADC then communicates its data via a serial link to the Mini Medusa.

Packaging the large number of sensors found in the R2 hands was accomplished by utilizing a network of distributed ADCs which digitize and serialize the data being sent upstream. This in turn enables the use of small connectors and localized wiring harnesses that make the system extremely modular and serviceable

## VI. CONTROL STRATEGY

A full discussion of this control law is available in [16]. The final control law is presented here, where the actuators implement an inner position control loop.

$$p_c = p - k_d \dot{p} + \begin{bmatrix} R \\ W \end{bmatrix}^T K_p \Delta \begin{pmatrix} \tau \\ t \end{pmatrix} \quad (1)$$

$p$  and  $p_c$  represent the actual and commanded positions for the actuators,  $R$  ( $n \times n+1$ ) represents the kinematic mapping from tendon tensions ( $f$ ) to joint torques ( $\tau$ ),  $W$  is a row matrix selected orthogonal to  $R$ ,  $t$  is a scalar measure of the internal tension on the tendon network ( $t = Wf$ ), and  $K_p$  and  $k_d$  are constant gains.

## VII. APPLICATIONS

The hand’s capability to achieve a wide range of grasps opens up a plethora of possible applications normally only performed by humans. These range from very dexterous tasks such as rotating a knob through active finger motion to subtle grasps used to grip flexible materials (Fig. 15). As learned with Robonaut 1[17], soft goods in the form of compliant, low and high friction gloves are critical to successfully achieve and maintain stable contact during manipulation (Fig. 15).



Fig. 15. R2 hand interacting with (a) basic knob and (b) space blanket

The R2 hand can work with a variety of both terrestrial and “space” tools. Fig. 16 shows the hand manipulating a standard, but by no means lightweight, commercial drill. The index finger has sufficient control to modulate drill speed during bolt tightening. Fig. 16 shows two R2 hands working together with a portable x-ray device used by NASA geologists. The current operational modes include teleoperation and set-points driven by application specific tasks.

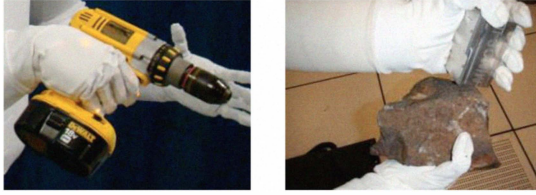


Fig. 16. R2 hand working with various devices, including (a) hand drill tool (b) portable x-ray device.

### VIII. LESSONS LEARNED

A key engineering development in the design of the R2 hand was the selection of the makeup of the braided polymer tendons. Spectra™ was initially chosen as the base tendon material for its high strength and favorable abrasion resistance characteristics. Unfortunately, it was determined early on that the creep inherent in Spectra™ cable is incompatible with the R2 finger actuation system, which has a finite travel of the ball screw actuator. Other high strength braided polymer cables were investigated, and Vectran™ was identified as a promising candidate. However, the lower abrasion resistance of Vectran™ cable posed a significant challenge.

To increase the abrasion resistance of the Vectran cable, PTFE strands were added to the braid. Exhaustive testing was performed to identify a combination of sliding surface material and tendon lubricant that would maximize the sliding life of the hybrid Vectran™ PTFE braid. It was concluded that leaded phosphor bronze along with Dupont Krytox™ lubricant significantly extended the abrasion life of the cable vs. other combinations tested. Bronze was subsequently incorporated into the sliding surfaces of the finger design, and tendons are pre-lubricated with Krytox™ prior to installation. Finally, the diameter of the tendon was increased by 50%, which increases the break strength to well above the required level, but also contributes substantially to abrasion life. The result is abrasion resistance of over 1 million cycles before failure in the experimental setup, an improvement of approximately five fold over the initial results.

### IX. CONCLUSIONS/FUTURE DEVELOPMENT

Research and engineering development on elements of the R2 hand are continuing in various phases of planning and design. Future work includes adaptation of Series Elastic Actuation, employed throughout Robonaut 2's upper arms and torso, for use in the lower arm wrist mechanism. Refinements to the robots "skin" for better grasping are being planned - improved "flesh," as well as tighter integration of the robot's soft goods with its mechanisms are design goals. Design concepts for additional passive degrees of freedom in the fingers are close to realizing initial prototypes. The need for smaller actuation, and for actuation not limited by finite travel of the motor ball screw arrangement, provide a wealth of opportunity for further innovation.

In conclusion, the Robonaut 2 hand greatly improves upon the capabilities of its predecessor in the areas of strength,

speed, sensing, and the ability to approximate human grasps. NASA and GM are both actively identifying applications where these capabilities can be exploited to the benefit of their human workforce. Together the organizations are also developing potential spinoffs that will make use of the technologies advanced in the R2 hand for applications outside the realm of traditional robotics.

### ACKNOWLEDGMENT

This work represents the effort of a community of researchers, and the authors would like to thank them for their technical excellence which produced the R2 hand.

### REFERENCES

- [1] Lovchik, C.S. and Diftler, M.A. "The Robonaut Hand: a Dexterous Robot Hand for Space." *Proceedings of the IEEE International Conference on Robotics and Automation*, Detroit, MI. pp. 907-912, 1999.
- [2] Kaneko, K., et al. "Humanoid Robot HRP-3." *Proceedings of the IEEE/RSJ International Conference on Intelligent Robots and Systems*, Nice, France, pp. 2471-2478, 2008
- [3] Akin, D.L., et al. "Development of a Four-Fingered Dexterous Robot End Effector For Space Operations." *Proceedings of the IEEE International Conference on Robotics and Automation*, Washington, DC, pp. 2302-2308, 2002
- [4] Grebenstein, M. et al. "Antagonistically Driven Finger Design for the Anthropomorphic DLR Hand Arm System." *Proceedings of the IEEE-RAS International Conference on Humanoid Robots*, Nashville, TN, USA, D. pp. 609-616, 2010.
- [5] Haidacher, S. et al. "DLR Hand II: Hard- and Software Architecture for Information Processing." *Proceedings of the IEEE International Conference on Robotics and Automation*, Taipei, Taiwan, pp. 684-689, 2003
- [6] Chen, Z., et al. "Experimental Study on Impedance Control for the Five-Finger Dexterous Robot Hand DLR-HIT II." *Proceedings of the IEEE/RSJ International Conference on Intelligent Robots and Systems*, Taipei, Taiwan, pp. 5867-5874, 2010
- [7] Cutkosky, M. "On Grasp Choice, Grasp Models, and the Design of Hands for Manufacturing Tasks." *Proc. of the IEEE Transactions on Robotics and Automation*, vol. 5, iss. 3, pp. 269-279. June 1989.
- [8] Diftler, M.A., et al. "Robonaut 2- The First Humanoid Robot in Space" *Proceedings of the IEEE International Conference of Robotics and Automation*, Shanghai China. pp 2178 - 2183, 2011.
- [9] 1988 Anthropometric Survey of U.S. Army Personnel: Methods and Summary Statistics, United States Army Natick Research, Development and Engineering Center, Natick Mass, September 1989
- [10] Salisbury, J. K., & Mason, M. T., *Robot Hands and the Mechanics of Manipulation*. MIT Press, Cambridge, MA, 1985.
- [11] Chang, L. and Matsuoka, Y. "A Kinematic Thumb Model for the ACT Hand." *Proceedings of the IEEE International Conference on Robotics and Automation*, Orlando, Florida, pp. 1000-1005, 2006
- [12] Ihrke, C., et al. "Bidirectional Tendon Terminator." US Patent Application 12/269,579, May 2010.
- [13] Ihrke, C., et al. "Robotic Thumb Assembly." US Patent Application 12/564,085, Mar 2011.
- [14] Ihrke, C., et al. "Phalange Tactile Load Cell." US Patent 7,784,363, August 2010.
- [15] Abdallah, M., et al. "Sensing the Tendon Tension Through the Conduit Reaction Forces." US Patent Application 12/269,552, May 2010.
- [16] Abdallah, M. Platt, R. Wampler, C. Hargrave, B. "Applied Joint-Space Torque and Stiffness Control of Tendon-Driven Fingers," IEEE-RAS Intl. Conf. on Humanoid Robots, Nashville, TN 2010.
- [17] Martin, T., et al "Tactile Gloves for Autonomous Grasping with the NASA/ DARPA Robonaut". *Proceedings of the IEEE International Conference on Robotics and Automation*, New Orleans, LA. pp.1713 - 1718 Vol.2 2004